Size fractionation upon adsorption of fulvic acid on goethite: Equilibrium and kinetic studies

QUNHUI ZHOU,[1] PATRICIA A. MAURICE,[2,*] and STEPHEN E. CABANISS[3]

[1]Department of Geology, Kent State University, Kent, Ohio 44242, USA
[2]Department of Civil Engineering and Geological Sciences, University of Notre Dame, Notre Dame, Indiana 46556, USA
[3]Department of Chemistry, Kent State University, Kent, Ohio 44242, USA

Abstract—We examined adsorption equilibrium and kinetics of an aquatic fulvic acid (XAD-8 resin extract) onto goethite (α-FeOOH). Molecular weight distributions were determined using high-pressure size exclusion chromatography (HPSEC). Overall adsorption isotherms and those of the most abundant intermediate molecular weight (IMW) fraction (1250–3750 Da) fit the Langmuir adsorption equation, as is commonly observed for humic substances. However, this overall fit masked the non-Langmuir isotherm shape of high and low molecular weight (HMW, LMW, respectively) fractions. We observed preferential adsorption of HMW fractions at low pH and of IMW fractions at higher pH. We also observed preferential adsorption of components with higher absorbance normalized to moles C (ε_{280}), probably reflecting greater aromaticity. Over the first 6 h of adsorption experiments, adsorbed organic carbon increased and weight average molecular weight (M_w) of the organic matter remaining in solution decreased, consistent with slower adsorption of higher molecular weight components. Observations of fractionation upon adsorption agreed well with a field study showing lower M_w and lower ε_{280} organic matter in deeper ground water relative to surface and shallow ground water. *Copyright © 2001 Elsevier Science Ltd*

1. INTRODUCTION

Adsorption of natural organic matter (NOM) onto mineral surfaces modifies mineral surface properties and reactivity (Tipping, 1981; Tipping and Cooke, 1982; Liang and Morgan, 1990; Murphy et al., 1990; Ochs et al., 1994; Stevenson, 1994; Vermeer et al., 1998) and strongly influences the fates of contaminants and other species in soils, aquifers, and surface-water environments (Davis, 1982; Chiou et al., 1986; Cabaniss and Shuman, 1988; Murphy et al., 1990; 1992; Gu et al., 1994; 1996; Vermeer et al., 1998). A quantitative understanding of the adsorption of humic substances (HS), the predominant components of NOM, onto mineral surfaces is prerequisite for developing predictive models of contaminant mobility. Yet, a quantitative understanding has remained elusive because HS are by definition polydisperse mixtures of heterogeneous poly-electrolytes (Stevenson, 1994; Vermeer and Koopal, 1998) with variable composition, molecular weight (MW) and functionality.

HS exhibit some of the same adsorption characteristics observed for polydisperse polymer adsorption, including isotherms that depend on sorbent surface-area-to-volume ratio, and adsorption–desorption hysteresis (Koopal, 1981; Vermeer et al., 1998). Hence, we may gain some insight into HS adsorption from the polymer literature. For nonionic polymers, preferential adsorption of high molecular weight (HMW) fractions over low molecular weight (LMW) fractions and displacement of fast-adsorbing LMW fractions by thermodynamically favored HMW fractions have been demonstrated both experimentally and theoretically (Cohen Stuart et al., 1980; Koopal, 1981; Kawaguchi, 1990). Polyelectrolyte adsorption is similar, but more complex. Polyion charge, adsorbent surface charge, ionic strength, and pH exert additional influences on adsorption (Kawaguchi, 1990; de Laat et al., 1995; de Laat and van den Heuvel, 1993; 1995). de Laat et al. (1995), in a study of polyacrylic acid (PAA) salts adsorption on BaTiO$_3$, observed preferential adsorption not of HMW fractions but rather of intermediate molecular weight (IMW) fractions. They suggested that adsorption of HMW components was inhibited by an electrostatic barrier at the interface that increased with molecular size (larger molecules having higher total charge) and decreased with increasing ionic strength. Once the mineral surface became covered with PAA, its negative charge would cause an electrostatic barrier to adsorption of large, highly charged PAA molecules.

For NOM, research by several groups has suggested preferential adsorption of certain components: HMW fractions (Tomaic and Zutic, 1988; Ochs et al., 1994; Wang et al., 1997; Meier et al., 1999; Namjesnik-Dejanovic et al., 2000), IMW fractions (Davis and Gloor, 1981), aromatic moieties (McKnight et al., 1992), and/or hydrophobic components (McKnight et al., 1992; Gu et al., 1995; Chin et al., 1997). HS also display adsorption–desorption hysteresis even after days or weeks, suggesting that adsorption equilibrium is not attained (Gu et al., 1994; 1996). Although it is very difficult when dealing with humic substances to identify equilibrium, it is important to establish whether a steady state is attained in order to properly analyze isotherm properties. Vermeer and Koopal (1998) and Avena and Koopal (1999) reported that HS adsorption proceeds by a quick initial adsorption process (80–100 seconds), followed by a slow rearrangement of the adsorbed layer either through conformational changes or by replacement of adsorbed molecules with new attaching molecules. For polydisperse HS, this latter process may continue for many hours.

Difficulties encountered in modeling adsorption of synthetic

---

* Author to whom correspondence should be addressed (pmaurice@nd.edu).

Table 1. Mean of M_n, M_w, and molar absorptivity (ε_{280}) of FA (NJ) at different pH, 0.01 M NaCl, and 2.5 to 40 mg C L^{-1}. The number in parentheses is the standard deviation.

pH	M_n	M_w	M_w/M_n	ε_{280}	No. of samples
3.5	1310 (80)	2130 (40)	1.63 (0.08)	430 (2)*	8
5.5	1370 (60)	2250 (30)	1.64 (0.07)	451 (15)	17
7.5	1420 (80)	2290 (40)	1.60 (0.05)	472 (11)	18
5.5 and 7.5	1420 (80)	2270 (40)	1.61 (0.03)	460 (18)	35
3.5, 5.5, and 7.5	1390 (90)	2230 (80)	1.61 (0.08)	458 (18)**	43

* 3 samples.
** 38 samples.

polyelectrolytes are greatly amplified when dealing with highly complex and variable NOM. Hence, empirical and data-fitting models have become popular for describing NOM adsorption. However, a molecular-based understanding of NOM adsorption requires more detailed studies.

In this paper, we combine steady-state (24 h reaction) and kinetic adsorption studies with MW analysis by high pressure size exclusion chromatography (HPSEC; Zhou et al., 2000) and estimation of aromaticity using UV/Visible spectrophotometry to (1) characterize adsorption isotherms of FA on goethite; (2) directly measure changes in MW and absorbance normalized to moles *C* upon adsorption (i.e., fractionation); and (3) monitor the progress of adsorption and fractionation over time. We further compare the results of batch adsorption/fractionation experiments with observed changes in the NOM pool in a small freshwater wetland.

2. MATERIALS AND METHODS

2.1. Mineralogical Sample

Goethite (α-FeOOH) was chosen as the sorbent because of its widespread abundance, its stability and its strong NOM adsorption over a range of solution conditions. Goethite was synthesized following the procedure of Schwertmann and Cornell (1991, p. 64). X-ray diffraction analysis showed synthetic goethite with no detectable crystalline impurities. The BET specific surface area (A_S) was determined by N_2 adsorption to be 26.8 ± 0.2 m^2 g^{-1}. Atomic-force microscopy (AFM) showed that individual goethite particles were acicular (needle shaped) with approximate average dimensions of $1500 \times 150 \times 40$ nm; most particles were 1000 to 3000 nm long. Larger particles had a composite micromorphology consisting of parallel domains (elongated along *c* axis) of unequal length and width, with individual domains bounded mostly by (110) faces (Schwertmann and Cornell, 1991; Fischer et al., 1996). From particle dimensions, we calculated a geometric surface area of $\sim$12 m^2 g^{-1}; microtopography introduced by numerous domains apparently contributed to the higher BET measured surface area. For each of the adsorption experiments described below, a goethite stock solution (8.942 g L^{-1}) was made up in MilliQ ultraviolet (UV) treated water and stirred for $\sim$1 h prior to use.

2.2. NOM Samples

NOM-rich surface water was collected at McDonalds Branch Basin, a freshwater wetland in the New Jersey Pine Barrens, USA (for site description, see Johnsson and Barringer, 1989; Meier et al., 1999). The surface water was filtered through 0.45 μm silver membrane filters and stored in the dark at 4°C. Dissolved organic carbon concentration (DOC) and pH were 24.2 mg C L^{-1} and 3.8, respectively. FA was isolated using a modification of the XAD-8 procedure described by Aiken et al. (1992), in Aiken's USGS laboratory. The elemental composition of the FA was determined (Huffman Labs, Golden, CO) to be C 46.35%, H 4.27%, O 45.60%, N 0.44%, and S 0.49%. The atomic

ratio of O/C, 0.74, is considerably higher than the average value of $\sim$0.60 for aquatic FAs reported by Steelink (1985), which suggests that this FA is highly polar.

Traina et al. (1990) and Chin et al. (1994) reported that the aromaticity (% aromatic C by ^{13}C NMR) of HS is proportional to their absorbance at 280 nm normalized to moles C (ε_{280}). The number average molecular weight (M_n), weight average molecular weight (M_w), and ε_{280} of the FA are shown in Table 1. The ε_{280} of the FA falls in the upper part of the range 100–500 L (mole C)$^{-1}$ cm^{-1} that Chin et al. (1994) reported for aquatic fulvic acids. M_n and M_w were measured by HPSEC by our group to be 1386 ± 95 and 2230 ± 80 Da, respectively, and are also higher than those of many aquatic FAs.

2.3. Adsorption Experiments

2.3.1. Steady-state adsorption isotherm

Adsorption experiments were conducted at pH 3.5, 5.5, and 7.5, in 28 mL polycarbonate centrifuge tubes at 22 ± 1°C with 20 m^2 L^{-1} of goethite at each pH. Taking pH 3.5 as an example, a stock solution of FA (30–50 mg C L^{-1}) was prepared by adding freeze-dried solid FA and 0.01 M NaCl into MilliQ ultraviolet (UV) treated water and storing in a refrigerator at 4°C overnight to permit full hydration. On the next day, the stock solution was adjusted to pH 3.5 using NaOH and HCl. A 0.01 M NaCl blank solution was prepared by adding NaCl to MilliQ UV water and adjusting pH to 3.5. Next, 75 mL of 0 to $\sim$40 mg C L^{-1} sample solutions were made up in flasks by mixing different proportions of blank and FA stock solutions volumetrically, after which pH was adjusted, if needed, to 3.5. The procedure for solution preparation at pH 5.5 and 7.5 was the same as for pH 3.5, but 0 to $\sim$35 and 0 to $\sim$30 mg C L^{-1} sample solutions were prepared for pH 5.5 and 7.5, respectively. Each sample solution was split into three polycarbonate centrifuge tubes (22 mL in each). 2 mL of the goethite stock suspension was added to each of the first two tubes and 2 mL MilliQ UV water was added to the third tube as a control sample without goethite. In the discussion below, we refer to "control" samples as samples containing NOM but not containing goethite.

After shaking for 24 h in the dark, samples were centrifuged 15 min at 13,500 rpm (Marathon 21000R, Fisher). 18 mL of supernatant were removed into Teflon® beakers and filtered through 0.1 μm Nuclepore® polycarbonate membranes. The filtrate was split into three sample bottles for DOC (in glass), Fe (in high density polyethylene HDPE), UV/Vis and HPSEC (in glass) analyses. DOC and Fe samples were acidified to pH $\sim$2.0 by adding ultrapure concentrated HCl (Aldrich, 99.999%+ purity). Preliminary work using unfiltered samples showed that 2–3% of fine goethite particles remained in the separated supernatants at low DOC and low pH or at high DOC and high pH. This problem was similar to that reported by Tipping (1981) and Gu et al. (1994). The presence of the fine particles in some samples can influence Fe, UV, and DOC analyses. Hence, we added the filtration step. Controls were treated in the same manner as samples, throughout. No significant difference of DOC, Fe, ε_{280}, MW, and molecular weight distribution (MWD) between filtered and unfiltered controls was detected.

2.3.2. Kinetic experiments

DOC concentrations for kinetic experiments were chosen based on the adsorption isotherms and MW fractionation data resulting from experiments described above. We chose ~23 mg C L^{-1} as a starting concentration for kinetic experiments because this starting concentration resulted in a point near the middle of the plateau of the adsorption isotherms for all three pHs. As will be clear from our discussion below, MW fractionation or displacement over time was expected to be most likely and prominent at this DOC concentration. In order to keep the same DOC concentration and ionic strength for each pH, a 0.01 M NaCl and ~25 mg C L^{-1} stock FA solution was made and stored in the refrigerator overnight. The next morning, the stock solution was split into three beakers, and pH adjusted to 3.5, 5.5, and 7.5, respectively. Samples were made up to 24 mL volume (22 mL stock solution plus 2 mL goethite stock suspension or 2 mL MilliQ UV water) and 20 m^2 L^{-1} goethite suspension (or nongoethite controls) in centrifuge tubes and shaken at 22 ± 1°C in the dark. For each pH, we removed duplicate samples at 15 min, 30 min, 1.25, 3, 6, 12, 24, 48, and 72 h. Control samples (not reacted with goethite) were removed at 15 min, 24 h, and 72 h. Processing of samples was the same as for the adsorption isotherm experiments described above.

2.3.3. DOC, UV/Visible spectrophotometry and Fe analyses

DOC was analyzed in triplicate on a Shimadzu TOC-5000 analyzer. The relative standard deviation (RSD) was ≤2% for DOC > 2 mg C L^{-1}, and ≤5% for DOC ≤ 2 mg C L^{-1}. The amount of NOM adsorbed ($C_{adsorbed} = q = \Gamma$) was calculated from the difference between the initial (C_0, control, before adsorption) and final ($C_{aq} = C$, after adsorption) DOC. UV/Visible absorbance spectra of NOM were collected on a Hitachi U2000 double-beam spectrophotometer using 1 cm quartz cells with MilliQ UV water as the reference, scanned from 600 to 200 nm at 100 nm min^{-1}. The absorbance at 280 nm was used to determine ε_{280} [$\varepsilon_{280} = A_{280}/DOC$, with units L (mole C)$^{-1}$ cm^{-1}] of organic matter in solution. Dissolved Fe was measured with a Perkin Elmer 5100 PC graphite furnace atomic absorption spectrophotometer (GFAAS).

2.3.4. Langmuir equation parameters

To provide convenient parameters for comparing isotherms, FA adsorption data were fitted to the Langmuir equation

$$q = \Gamma = \frac{K_q q_m C}{1 + K_q C}, \tag{1}$$

where q is the adsorbed density (mg C m^{-2}) on the surface, q_m is the maximum adsorbed density, K_q [L (mg C)$^{-1}$] is the adsorption equilibrium constant, and C (mg C L^{-1}) is the equilibrium concentration of NOM in solution. For these data, q_m is well determined by the isotherm plateau, while K_q typically is determined from q_m and the first few low-DOC data points. Use of the Langmuir equation for this purpose does not imply that all assumptions (e.g., Stumm, 1992) of the model apply.

2.4. Determination of MW and MWD

2.4.1. HPSEC method

HPSEC was used to determine the MW distribution (MWD) and average MW of NOM before and after reaction with goethite. A detailed description of the HPSEC method is provided elsewhere (Chin et al., 1994, as modified by Zhou et al., 2000). The Waters HPSEC instrumentation included an HPLC pump, 600E system controller, 994 programmable photodiode array detector, 712 WISP™ autosampler equipped with a 1–2000 μL sample loop, temperature control module with column heater, and Baseline 810 chromatography workstation (Waters Associates). The system used a Waters Protein-Pak 125 modified silica column (30 mm long, 7.8 mm diameter) and simultaneous detection wavelengths = 215, 230, 254, and 280 nm. The mobile phase consisted of 0.1 M NaCl in MilliQ water with 4 mM phosphate buffer (pH 6.8). Sodium polystyrene sulfonates (PSS) with M_n = 18 K, 8 K, 5.4 K, 4.6 K (Polysciences), salicylic acid (MW = 138, 99.999% purity, Aldrich) and acetone (MW = 58, HPLC grade, Aldrich) were used as standards (Zhou et al., 2000). The calibration curves of the HPSEC systems were constructed by determining the peak retention times of standards with narrow MWD. The HPSEC is subject to a 3–5% daily deviation of average MW when applied to humic substances (Zhou et al., 2000).

2.4.2. Calculating MW distributions and averages

The molecular weight distribution (MWD) and average molecular weights of both adsorbed and nonadsorbed organic matter must be calculated in order to study the MW dependence of adsorption. To calculate a MWD (molecular frequency as a function of molecular weight) from an experimental HPSEC chromatogram (absorbance as a function of retention time), we must convert both retention time to molecular weight and absorbance to molecular frequency (or mass frequency). Retention time is readily converted to molecular weight using a calibration curve, but converting absorbance to molecular frequency requires additional information or assumptions.

Typically, the absorbance of an NOM solution is assumed to be proportional to the DOC, so the constant of proportionality need not be known to calculate the number average molecular weight (M_n) and the weight average molecular weight (M_w) from HPSEC chromatograms using standard equations (Yau et al., 1979; Chin et al., 1994; Zhou et al., 2000). In the case of adsorption experiments, however, the constant of proportionality (k) is not the same for the control (whole NOM) samples as for the fractionated NOM remaining in solution after adsorption (see below). To compare the MWD of adsorbed and nonadsorbed NOM on a DOC basis, it was necessary to correct the absorbance data by normalizing chromatogram peak area (i.e., integrated absorbance) to DOC. Once normalized, the resulting MWD of organic carbon versus molecular weight can be calculated for the controls and for the nonadsorbed NOM, and the MWD of adsorbed NOM is calculated by difference. For the ith molecular weight interval in the chromatogram,

$$C_{i,ads} = C_{i,control} - C_{i,solution} = A_{i,control}/k_{control} - A_{i,solution}/k_{solution}, \tag{2}$$

where $A_{i,control}$ and $A_{i,solution}$ are the absorbances of the ith interval and $k_{control}$ and $k_{solution}$ are the constants of proportionality for the controls and the solutions remaining after adsorption. The results of this calculation are shown in the insets of Figure 1. This procedure corrects for differences in average k between samples but not for changes in k as a function of MW within a sample. This method thus ensures mass balance with respect to organic C, but still is an approximation of the complex relationships between absorbance and NOM properties.

For some purposes, it is convenient to represent the continuous MWD as a small number of discrete fractions, each representing a range of MW. We divided the log MWD into six fractions between 50 and 18,000 Da and calculated the area of each fraction in the chromatograms before and after adsorption. The NOM in the jth MW fraction which adsorbed to the surface, $f_{j,ads}$, is given by Eqn. (3),

$$f_{j,ads} = f_{j,control} - f_{j,solution}, \tag{3}$$

where f represents the DOC in the MW fraction j and other subscripts retain the meaning above.

3. RESULTS AND DISCUSSION

3.1. Adsorption Isotherms

Adsorption appeared to reach a steady state by 24 h (see Sect. 3.5 below); hence, we present steady state adsorption isotherms in Figure 1. The adsorption isotherms (Fig. 1) at all three pH values showed a steep initial slope (at low equilibrium DOCs) that reached a plateau as equilibrium C concentration increased. This general isotherm shape indicates high affinity interaction of the NOM with the sorbent and a finite sorption capacity (Sposito, 1984; Gu et al., 1994), and commonly is observed for adsorption of HS on Fe(III)(hydro)oxides. Sorp-
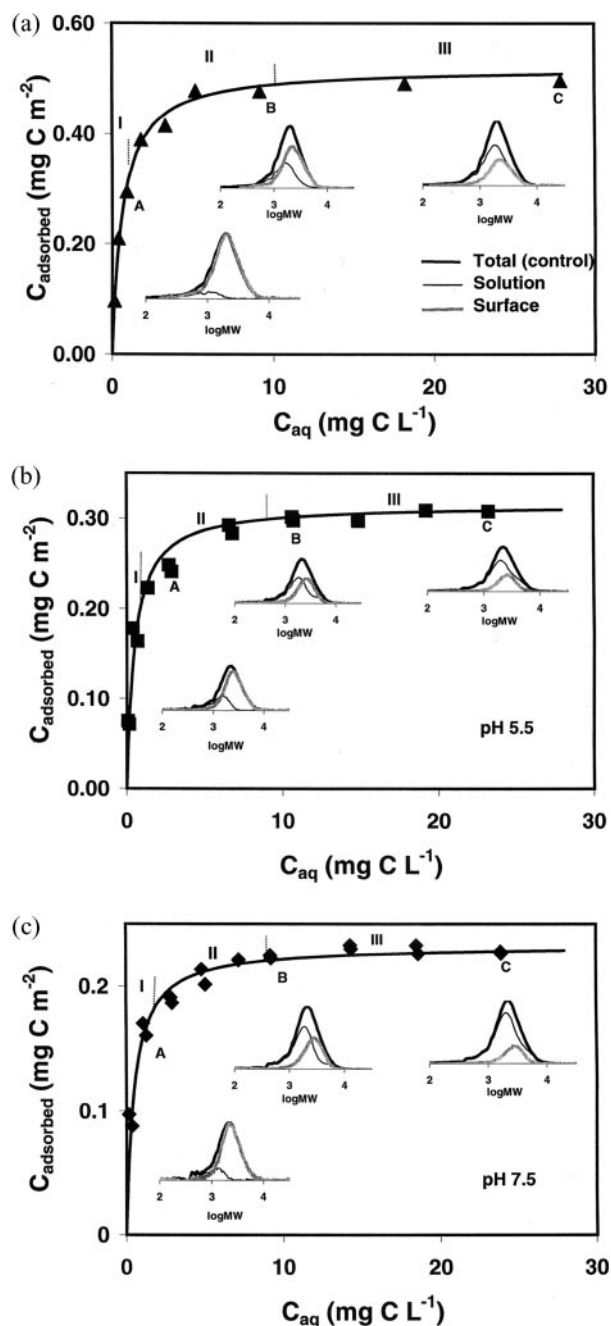
Fig. 1. Adsorption isotherms and molecular weight distribution (MWD) of FA in 0.01 M NaCl, 22 ± 1°C, 20 m^2 L^{-1} goethite, at pH 3.5 (a), 5.5 (b), and 7.5 (c). Adsorption isotherms follow the Langmuir model (solid line over concentration, Langmuir parameters are shown in Table 2). MWD under the isotherm show preferential adsorption of IMW–HMW, where wide black, narrow black, and gray lines mark the MWD before adsorption (control), remaining in solution following adsorption, and adsorbed on the surface, respectively. Capital letters A, B, and C represent the sample position of MWD. Areas I, II, and III are separated by the vertical dotted lines. Error bars on MWD plots are within the width of the lines.

tion capacity, expressed as the Langmuir parameter q_m noticeably decreased with increasing pH (Table 2), in agreement with previous observations (Tipping, 1981; Gu et al., 1994; 1995).

The high adsorption capacity at pH 3.5 is likely due (a) to high density of surface reactive sites (>Fe–OH$_2^+$, >Fe–OH), which may bind NOM through ligand exchange, and (b) to relatively weak electrostatic repulsion between molecules. Additionally, in-solution atomic force microscopy (AFM) of HS on muscovite and hematite surfaces suggests that conformational changes may result in less tight packing of adsorbed HS as pH increases (Maurice and Namjnesnik-Dejanovic, 1999; Namjnesnik-Dejanovic and Maurice, in press).

In agreement with previous research (e.g., Parfitt et al., 1977; Tipping, 1981; Davis, 1982; Murphy et al., 1992; Gu et al., 1994; Wang et al., 1997) the adsorption isotherms at each pH showed good fits to the Langmuir equation (solid lines in Figures 1a–c), although this goodness of fit should not be taken to imply that NOM adsorption fits the assumptions of the Langmuir model (see Sposito, 1984; Stumm, 1992).

In-solution AFM suggests that HS adsorb as spheres at pH ~3. Assuming that a FA molecule adsorbs on the surface as an ideal sphere with average M_n ~1400 Da and 46.5% O, the calculated covered area per molecule would be πr^2 if the spheres pack tightly as a monolayer. A 22 to 13 O atoms/nm^2 density is calculated if $r = 0.77$ nm (Aiken and Malcolm, 1987) to 1 nm (measured by AFM by Maurice and Namjesnik-Dejanovic, 1999 and Namjesnik-Dejanovic and Maurice, in press), respectively. These calculated values are very close to the experimental results at pH 3.5 (Table 2), suggesting that monolayer adsorption is achieved at the observed adsorption maximum. In agreement with in-solution AFM images, however, this monolayer would not consist of flat-lying molecules spread out on the surface but rather of spherical-shaped molecules with only some functional groups contacting the surface (Ghabbour et al., 1998).

3.2. Preferential Adsorption

The adsorption isotherms shown in Figure 1 can be divided into three areas (I, II, III) in terms of MWD characteristics, the average MW fractionation between surface and solution, and surface coverage, θ ($=C_{ads}/q_m$). Area I is the steep upward sloping portion of the isotherm, $\theta \leq 0.75$. In area II, the slope of the isotherm decreases, $0.75 < \theta < 0.97$. Area III represents the start of the adsorption isotherm plateau, $\theta \geq 0.97$.

The three areas defined by our data can be compared with the three regions of adsorption isotherms theoretically predicted by Cohen Stuart et al. (1980) for a binary mixture of nonionic monopolymers with different chain length. In their region I (similar to our area I), all molecules adsorbed and no competition or displacement occurred because of the low density of occupied surface sites. The polymers that they used were of relatively high affinity, i.e., likely to adsorb; very low affinity molecules might not adsorb even in the absence of competition. Our area I was broadly similar but it differed in that a portion of LMW molecules did not adsorb. In their region II (which corresponded to our area II), all large molecules and a portion of smaller molecules adsorbed; they suggested that some small molecules remained in solution because of competition with the HMW polymer which adsorbed completely and preferentially. Our area II agreed with this model. In their region III, the adsorption plateau, sorbate molecules greatly exceeded sorbent surface sites. Due to competition, only large molecules ad-

Table 2. Langmuir model parameters by fitting adsorption isotherm data.

pH	K_q (m³/g)	q_m			ΔG^0_{ads} (kJ mol⁻¹)	R^2
		mg C m⁻²	C atoms nm⁻²	O atoms nm⁻²		
3.5	1.6	0.52	26	19	−35	0.9965
5.5	2.0	0.32	16	12	−36	0.9581
7.5	2.0	0.23	12	8.7	−36	0.9855

sorbed and all small molecules remained in solution. Our area III generally agrees with this model, but there is again a portion of HMW molecules that does not adsorb and the relative importance of this nonadsorbing HMW component is greater than in area II.

It is perhaps not surprising that our system is broadly similar to the predictions of Cohen-Stuart et al. (1980), but with some important differences. In their study, the two different chain-length polymers had the same chemical composition and nonionic structure. For a polyelectrolyte, preferential adsorption is affected not only by chain length but also by the charges of sorbent and sorbate, the pH, the ionic strength (our system maintained constant ionic strength 0.01 M), and the chemical compositions and structures of the different chemical components (Kawaguchi, 1990; Fleer et al., 1993). HS have been shown to have a range of MWs, structures, and functional groups and hence should not be expected to fit a simple model.

Fig. 2. Distribution of molecular weight averages with equilibrium DOC of solution (C_{aq}). (a) is MW average remaining in solution at three pHs; (b) is MW average adsorbed on the surface at pH 7.5.

Nonetheless, the comparison of our data with the Cohen Stuart et al. (1980) model suggests that molecular size exerts an important but not exclusive control on competitive adsorption behavior.

One explanation for the preferential adsorption of the IMW-to-HMW fractions and the perhaps unexpected observations that (1) some LMW material appears to be nonadsorbing even in area I and (2) some HMW material does not adsorb preferentially in area III may lie in the chemical structures of the molecules. For example, a portion of the LMW and/or HMW fractions may contain a type or number of functional group less conducive to adsorption. The polydisperse NOM samples are multicomponent mixtures rather than chemically pure substances.

Based on theoretical calculations and experimental observations of anionic polymer adsorption, de Laat et al. (1995) and de Laat and ven den Heuvel (1995) suggested that an electrostatic barrier may limit displacement of shorter chains by highly charged longer chains, leading to preferential adsorption of IMW fractions over HMW fractions. In our system, as pH increases from pH 3.5 to pH 7.5, the negative charge density on the NOM molecules increases, and the positive surface charge density on the goethite decreases (pH$_{pzc}$ of goethite = 8–10, Cornell and Schwertmann, 1996). The increasing electrostatic repulsion between neighboring negatively charged adsorbing molecules could potentially limit adsorption, and this effect would be greater for larger and more highly charged molecules. This might explain why a portion of the HMW fraction does not compete successfully for adsorption, especially at higher solution pH. We cannot evaluate whether larger molecules become sterically hindered from adsorbing at high pH because the effects of pH on steric properties are unknown.

Another possible explanation for the apparently anomalous behavior of the HMW fraction may lie in kinetic considerations if the system has not attained equilibrium by 24 h. Ochs et al. (1994) and Gu et al. (1995) proposed that fast-adsorbing LMW fractions are successively displaced by slow-adsorbing HMW fractions. Hence, it is possible that HMW molecules had not yet fully displaced IMW molecules in our system. However, this does not appear to be the case, as discussed in Sect. 3.5 below.

3.3. Fractionation of Molecular Weight and ε_{280}

Fractionation may be defined as the different partitioning of a physical and/or chemical property such as MW, acidity, aromaticity, and/or ε_{280} of NOM between different phases, in this case adsorbed versus dissolved. We observed fractionation in terms of average M_n, M_w, polydispersity (ρ), and ε_{280} upon adsorption of the FA onto goethite. The greatest amount of fractionation (biggest differences in solution M_n and M_w at a
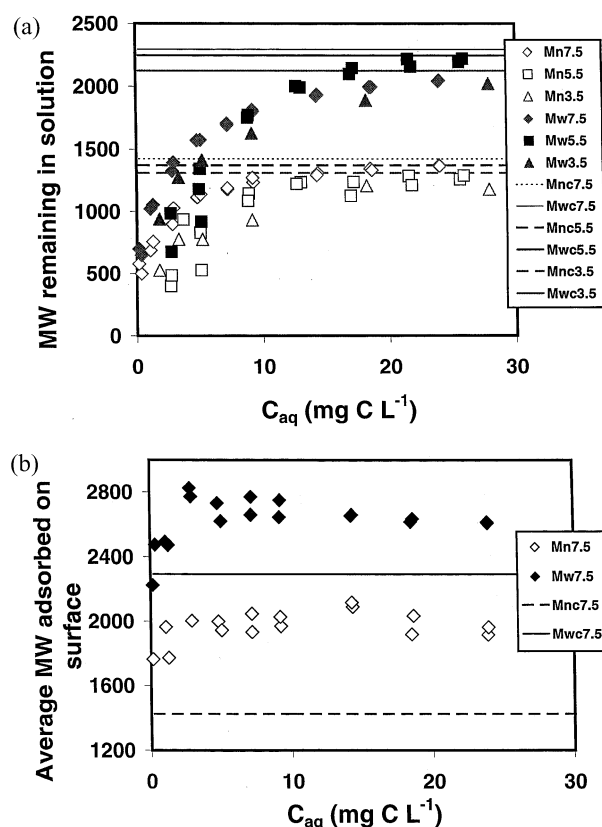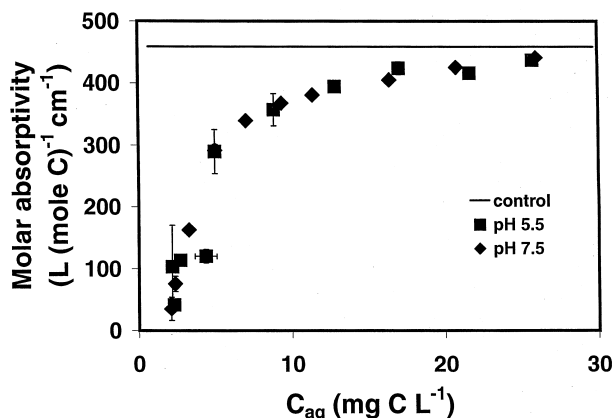
Fig. 3. Relationships of the absorbance normalized to moles C (ε_{280}) and equilibrium DOC of solution (C_{aq}) of FA at pH 5.5 and 7.5.

Fig. 4. Correlation between molecular weight averages and ε_{280} of the FA following adsorption. Linear functions are fitting data of both pH 5.5 and 7.5.

given DOC) occurred at pH = 3.5, which was also the pH of the maximum q_m.

Figure 2 shows the average MWs (M_n and M_w) remaining in solution and adsorbed on the surface as a function of DOC remaining in solution at 24 h reaction time. Both M_n and M_w of NOM remaining in solution following adsorption were lower than those before adsorption (control values, c) (Fig. 2a). M_n and M_w of NOM adsorbed on the surface were higher than control values (Fig. 2b). These data indicate preferential adsorption of large molecules, leading to fractionation. The extent of MW fractionation became smaller with increasing DOC in solution. The highest M_w on the surface (Fig. 2b) occurred in area II (see Fig. 1), which was the region showing strongest adsorption of the highest MW fraction. As noted above, the proportion of the highest MW fraction adsorbed on the surface in area II was greater than in area III. In area I (far left of Fig. 2b), nearly all molecules adsorbed (except for a small portion of the LMW fraction), and the M_w of NOM on the surface hence converged with the control solution.

We also observed that the ρ of NOM remaining in solution and adsorbed on the surface following adsorption tended to be less than that of the unreacted FA controls at all three pHs. This is consistent with fractionation upon adsorption.

Figure 3 shows the change in ε_{280} of FA upon adsorption at pH 5.5 and 7.5; data at pH 3.5 were likely strongly affected by relatively high Fe concentrations (as also observed by Maurice et al., 1998; Meier et al., 1999) and are not shown here. The ε_{280} values of all samples remaining in solution are lower than those of controls, which suggests preferential adsorption of more aromatic fractions onto goethite. Figure 4 shows linear relationships between M_w or M_n and ε_{280} for NOM remaining in solution following adsorption; this linear relationship suggests that the higher MW fractions include more aromatic moieties. The slope of M_w vs. ε_{280} in Figure 4 is the same as that reported by Chin et al. (1994) for a range of fulvic acids, but the intercept is smaller.

3.4. Adsorption Isotherms of Different MW Fractions

Adsorption isotherms for different MW fractions are shown in Figure 5. For all three pH values, fractions 3, 4, and 5
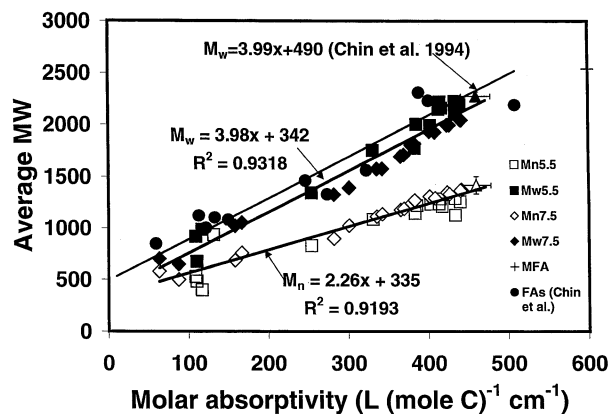
combined (mid 400s to 11,350 Da) contained 97% of the total mass (Table 3). At pH 5.5 and 7.5, essentially all of the lowest MW fractions 1 and 2 remained in solution. The adsorption behaviors of fractions 3, 4, and 5—especially fraction 4, which contained ~70% of the total mass—controlled overall adsorption. Adsorption of fraction 4 (1250–3750 Da) could be fit well by the Langmuir equation at all three pHs. The K_q of fraction 4 is larger than that of the total (all fractions combined), while the q_m is lower at all three pHs. Adsorption of other fractions could not be fit well by the Langmuir equation. At pH 7.5, for example, the R^2 for linear fits to the Langmuir model of fractions 3, 4, 5, and overall sample are 0.6046, 0.9098, 0.1837, and 0.9545, respectively. The isotherm shapes of high molecular weight material, fraction 5, at pH 5.5 and 7.5 (Fig. 5) showed an initial steep slope which reached a peak followed by a slight decrease. This suggests that the larger size HS molecules were excluded from the surface at high surface coverages. In contrast, fractions 3 and 4 attained a flat plateau. This suggests that a potential size and/or electrostatic barrier to adsorption only affects the larger molecules. Fractions 1, 2, and 6 represent such a small percentage of the total NOM that the isotherm shapes are difficult to evaluate.

The summed isotherms of fractions 4 and 5 yield a small step in area II, as do the overall adsorption isotherms (Fig. 1). Similar steps have been observed previously on NOM isotherms and attributed to potential changes in molecular orientation at the surface from flat lying to perpendicular to the surface (Ghabbour et al., 1998). Yet, in-solution AFM images do not support this theory (Maurice and Namjesnik-Dejanovic, 1999; Namjesnik-Dejanovic and Maurice, in press). Results of our adsorption/fractionation experiments suggest that the "steps" on the overall isotherms may be caused by the combination of differently shaped isotherms of different MW fractions.

The Langmuir shape of the overall adsorption isotherms is therefore dominated by the IMW components, those in fraction 4, and this fraction obscures non-Langmuirian behavior at higher and lower MWs. This might explain why so many previous researchers (Tipping, 1981; Davis, 1982; Murphy et al., 1992; Day et al., 1994; Gu et al., 1994; Wang et al., 1997; Namjesnik-Dejanovic et al., 2000) described Langmuir adsorp-
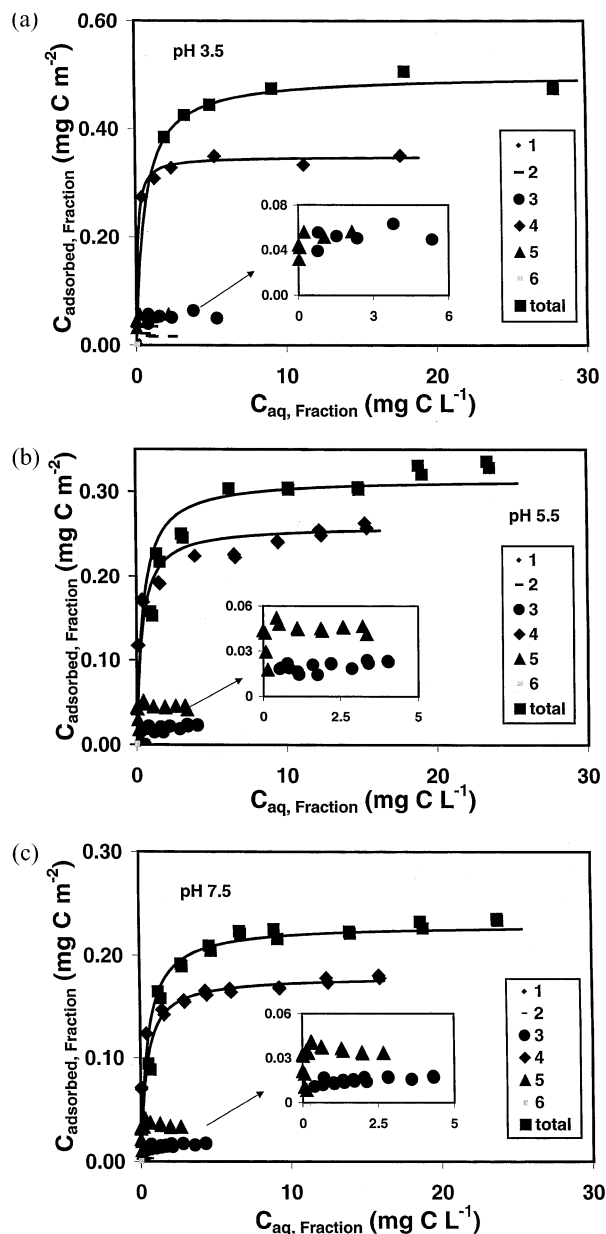
Fig. 5. Adsorption isotherms of different MW fractions on goethite. Solid lines were modeled by the Langmuir equation. The features of fractions are shown in Table 3.

tion for a wide variety of aqueous NOM samples. The most abundant fraction 4 can be assumed to behave as a monodisperse polymer based on the calculated polydispersity $M_w/M_n < 1.1$ (Table 3 shows an example at pH 7.5). The fraction of molecules with MW > 4500 Da occupied only ∼6.5% of the total mass. This is the size range that showed less adsorption at higher DOC values (pH 5.5 and 7.5).

Davis and Gloor (1981) used gel exclusion chromatography to determine MW distributions of NOM. They found that the fraction with MW 1000–3000 Da adsorbed most strongly among their three fractions (<500, 4000–500, >4000 Da). Our observation of strong adsorption by IMW fraction 4 (MW 1250–3750 Da) thus agrees quite well with their results, and provides more detailed fractionation data.

3.5. Adsorption and Fractionation Kinetics

We conducted kinetic experiments to determine the change of MW fractionation over time using the same electrolyte concentration (0.01 M NaCl) and pH values (3.5, 5.5, and 7.5) as described above. We selected an initial concentration of ∼23 mg C L^{-1} of FA because this concentration led to adsorption on the isotherm plateaus at all three pHs and because fractionation was observed at this concentration (see Fig. 1).

Previous researchers have reported NOM adsorption equilibration times of between a few minutes and a few hours (Davis and Gloor, 1981; Day et al., 1994; Ochs et al., 1994; Gu et al., 1994; 1995; Avena and Koopal, 1999). For our experiments (Fig. 6), overall adsorption (in terms of DOC) increased sharply during the first few hours and approached a steady state by ∼6 h. The adsorption rate at pH 3.5, 5.5, and 7.5 over the first 15 minutes is 1.39, 0.57, and 0.12 mg C m^{-2} h^{-1}, respectively. By 15 min reaction time, 74%, 63%, and 40% adsorption (relative to the amount at the steady state) was completed at pH 3.5, 5.5, and 7.5, respectively. Avena and Koopal (1999) observed a similar decrease in initial adsorption rate with increasing pH. Such a pH dependency of initial adsorption rate is likely related to pH effects on electrostatic forces and density of surface reactive sites. The fact that M_w reached steady state by 24 h suggests that the lack of adsorption of the highest MW fraction in area III (see Sect. 3.2) cannot be explained by slow adsorption kinetics of large molecules.

We observed evidence for replacement of lower MW molecules by higher MW molecules, even though we did not observe initial M_w higher than the control (unreacted NOM). The IMW to HMW fractions 4 and 5 remaining in solution following adsorption decreased over time. Avena and Koopal (1999) reported that the diffusion and attachment rates that control the initial adsorption rate of HS on hydrophilic surfaces

Table 3. Fraction features of FA (NJ) controls before adsorption at pH 7.5.

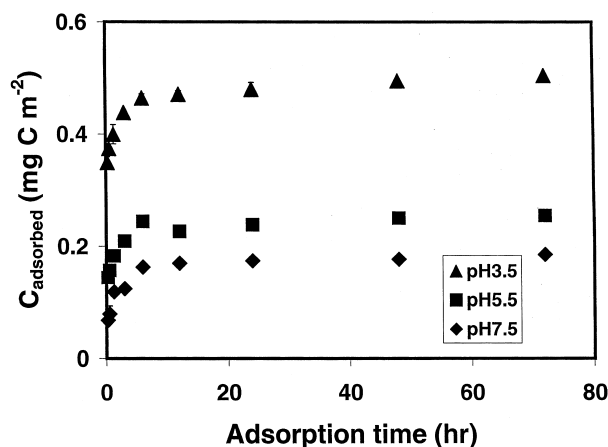| Fraction	Range of MW	M_w	M_n	P	% of the total
1	50–150	110	100	1.06	0.57
2	>150–450	320	290	1.11	2.14
3	>450–1250	920	800	1.14	16.72
4	>1250–3750	2280	2100	1.09	69.45
5	>3750–11,350	5000	4800	1.04	11.10
6	>11,350–18,450	13,670	13,530	1.01	0.03
Total	50–18,450	2290	1420	1.61	100

Fig. 6. Adsorption of FA on goethite over time using 23.19 mg C L^{-1} and 0.01 M NaCl solutions at pH 3.5, 5.5, and 7.5.

reach steady state in 80 to 100 seconds. Hence, it is possible that initial high M_w values occurred at <15 min reaction time, which was our first sampling interval. If a portion of lowest MW molecules is not capable of adsorption, as suggested by data in Figure 1, then the amount of any initial M_w increase in solution would be less than otherwise anticipated (i.e., still greater than control, but only slightly). Perhaps some of the fast adsorbed small molecules were still on the surface at 15 min but were gradually replaced by relatively larger molecules until 75 min. Then, the smaller molecules in solution penetrated the adsorbed layer to fill small spaces which could not be filled by large molecules due to the adsorbed molecules' rearrangement on the surface. This hypothesis might explain why the M_n remaining in solution tended to change from highest to lowest to medium over time (Fig. 7b).

3.6. Field Observation

The research described above is based on batch adsorption experiments, which are necessarily closed systems. Yet, many field situations are open systems wherein NOM can be continually resupplied (e.g., McCarthy et al., 1993). Nevertheless, the preferential adsorption that is quantified above may play a role in actual field situations.

Using additional samples collected at the McDonalds Branch stream (same location as samples used in batch experiments), we compared the MW characteristics of the bulk surface water with the surface water FA, a muck FA (MFA) extracted from the stream bed of this site, and shallow (5.5' deep) and deep (~20' deep) ground-water samples from beneath the stream bed (Fig. 8). The MW and ε_{280} in Figure 8 are in agreement with what would be expected if fractionation processes similar to those observed in the laboratory also occurred in the field. The relatively higher MW and more aromatic components are removed by the time that NOM reaches the shallow ground water at this site. Although the samples were not collected along a single flow path, they are representative of typical surface water, muck and ground-water samples in the basin. Preferential adsorption of relatively higher MW and/or higher aromatic components may be at least partially responsible for the FA properties in the muck layer.
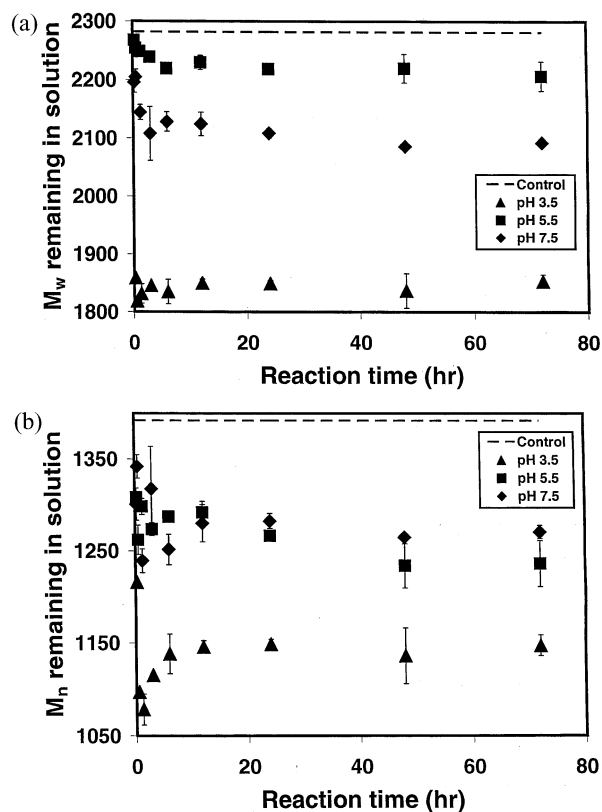

Fig. 7. Change of molecular weight averages in solution over time at pH 3.5, 5.5, and 7.5. Weight-average MW (a) and number-average MW (b).

McCarthy et al. (1993) injected NOM-rich water over the course of 2 weeks into a shallow, sandy coastal plain aquifer. The aquifer was in many respects similar to the field site we studied. Initially, they observed preferential adsorption/retardation of larger and more hydrophobic components along with greater mobility of smaller, more hydrophilic components. Eventually, however, NOM adsorption reached an apparent steady state such that the higher molecular weight, more hydrophobic components remained mobile in the aquifer. Our
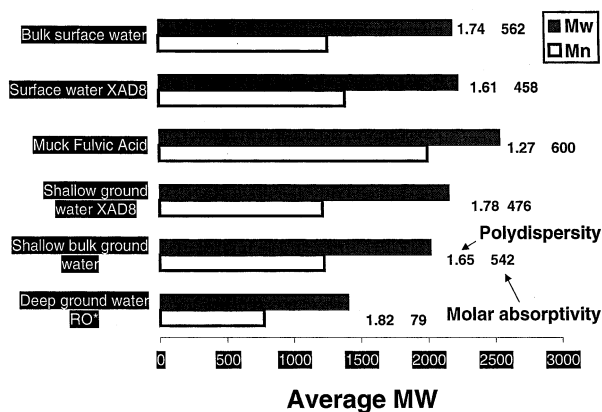

Fig. 8. Changes of M_n, M_w, and ε_{280} at site S2 (Johnsson and Barringer, 1989) in the New Jersey Pine Barrens.

results suggest that over the long term, the smaller and more aliphatic NOM components tend to be more mobile in the aquifer than the larger and more aromatic components. Hence, more detailed and long-term field studies, perhaps including variable hydrologic parameters, need to be conducted. Other processes such as microbial degradation may be important in the field and warrant further investigation.

4. SUMMARY AND CONCLUSIONS

1. In agreement with previous research, we observed that preferential adsorption resulted in a decrease in the molecular weight and aromaticity of NOM remaining in solution.

2. The Langmuir shape of the overall adsorption isotherm is dominated by the isotherm shape of the IMW molecules. The Langmuir isotherm shape of the IMW components, which are the most abundant, obscures non-Langmuirian isotherm shape at HMW and LMW.

3. We observed preferential adsorption of large molecules at low DOC and low pH and of IMW molecules at high DOC and higher pH. The preferential adsorption of IMW fractions may be related either to the limited density of surface sites and the great abundance of IMW molecules or the formation of an electrostatic barrier that is proportional to molecular size.

4. The preferential adsorption of higher MW and more aromatic components at pH $\sim$3.5 is consistent with observations of NOM properties in a small freshwater wetland.

5. Adsorption of FA on goethite reaches a steady state in 6–12 h with respect to DOC, M_n and M_w. We observed replacement of lower MW fractions by higher MW fractions.

Most models of polymer and polyelectrolyte adsorption do not take different proportions of organic components into consideration. We suggest that a model that includes polydispersity and polyelectrolyte effects may predict the adsorption behavior of NOM more effectively than the Langmuir approach alone; such modeling is the subject of our ongoing research.

REFERENCES

Aiken G. R., McKnight D. M., Thorn K. A., and Thurman E. M. (1992) Isolation of hydrophilic organic acids from water using nonionic macroporous resins. *Org. Geochem.* **18,** 567–573.

Avena M. J. and Koopal L. K. (1999) Kinetics of humic acid adsorption at solid-water interfaces. *Environ. Sci. Technol.* **33,** 2739–2744.

Cabaniss S. E. and Shuman M. S. (1988) Copper binding by dissolved organic matter: I. Suwannee River fulvic acid equilibria. *Geochim. Cosmochim. Acta* **52,** 185–193.

Chin Y.-P., Aiken G., and Danielsen K. M. (1997) Binding of pyrene to aquatic and commercial humic substances: the role of molecular weight and humic structure. *Environ. Sci. Technol.* **31,** 1630–1635.

Chin Y.-P., Aiken G., and O'Loughlin E. (1994) Molecular weight, polydispersity, and spectroscopic properties of aquatic humic substances. *Environ. Sci. Technol.* **28,** 1853–1858.

Chiou C. T., Malcolm R. T., Brinton T. I., and Kile D. E. (1986) Water solubility enhancement of some organic pollutants and pesticides by dissolved humic and fulvic acids. *Environ. Sci. Technol.* **20,** 502–508.

Cohen Stuart M. A., Scheutjens J. M. H. M., and Fleer G. J. (1980) Polydispersity effects and the interpretation of polymer adsorption isotherms. *J. Polymer Sci.* **18,** 559–573.

Cornell R. M. and Schwertmann U. (1996) *Iron Oxides: Structure, Properties, Reactions, Occurrence, and Uses*. VCH.

Davis J. A. (1982) Adsorption of natural dissolved organic matter at the oxide/water interface. *Geochim. Cosmochim. Acta* **46,** 2381–2393.

Davis J. A. and Gloor R. (1981) Adsorption of dissolved organics in lake water by aluminum oxide. Effect of molecular weight. *Environ. Sci. Technol.* **15,** 1223–1229.

Day G. M., Hart B. T., McKelvie I. D., and Beckett R. (1994) Adsorption of natural organic matter onto goethite. *Colloids Surf. A* **89,** 1–13.

de Laat A. W. M. and van den Heuvel G. L. T. (1993) Competitive and displacement adsorption of polyvinyl alcohol and the ammonium salt of a polyacrylic acid on $BaTiO_3$. *Colloids Surf. A* **70,** 179–187.

de Laat A. W. M. and van den Heuvel G. L. T. (1995) Molecular weight fractionation in the adsorption of polyacrylic acids onto $BaTiO_3$. *Colloids Surf. A* **98,** 53–59.

de Laat A. W. M. and van den Heuvel G. L. T., and Bohmer M. R. (1995) Kinetics aspects in the adsorption of polyacrylic acids onto $BaTiO_3$. *Colloids Surf. A* **98,** 61–71.

Fischer L., Muhlen E. Z., Brummer G. W., and Niehus H. (1996) Atomic force microscopy (AFM) investigations of the surface topography of a multidomain porous goethite. *Eur. J. Soil Sci.* **47,** 329–334.

Fleer G. J., Cohen Stuart M. A., Scheutjens J. M. H. M., Cosgrove T., and Vincent B. (1993) *Polymers at Interfaces*, 1st ed. Chapman & Hall.

Ghabbour E. A., Davies G., Goodwillie M. E., O'Donaughy K., and Smith T. L. (1998) Adsorption of humic acids on clays and minerals. 1. Adsorption of peat-plant- and soil-derived humic acids on kaolinite. *216th ACS National Meeting* **38(2),** 65–68.

Gu B., Mehlhorn T. L., Liang L., and McCarthy J. F. (1996) Competitive adsorption, displacement, and transport of organic matter on iron oxide: I. Competitive adsorption. *Geochim. Cosmochim. Acta* **60,** 1943–1950.

Gu B., Schmitt J., Chen Z., and McCarthy J. F. (1994) Adsorption and desorption of natural organic matter on iron oxide: mechanisms and models. *Environ. Sci. Technol.* **28,** 38–46.

Gu B., Schmitt J., Chen Z., Liang L., and McCarthy J. F. (1995) Adsorption and desorption of different organic matter fractions on iron oxide. *Geochim. Cosmochim. Acta* **59,** 219–229.

Johnsson P. A. and Barringer J. L. (1989) Water quality and hydrogeochemical processes in McDonalds Branch Basin, New Jersey Pinelands, 1984–88. USGS. Water Resources Investigation Report 91-4081.

Kawaguchi M. (1990) Sequential polymer adsorption—Competition and displacement process. *Adv. Colloids Interface Sci.* **32,** 1–41.

Koopal L. K. (1981) The effect of polymer polydispersity on the adsorption isotherm. *J. Colloid Interface Sci.* **83,** 116–129.

Liang L. and Morgan J. J. (1990) Chemical aspects of iron oxide coagulation in water: laboratory studies and implications for natural systems. *Aquatic Sci.* **52,** 32–55.

Maurice P. A., Namjesnik-Dejanovic K., Lower S. K., Pullin M. J., Chin Y.-P., and Aiken G. R. (1998) Sorption and fractionation of natural organic matter on kaolinite and goethite. In *Water-Rock Interaction IX* (eds. M. Arehart and N. Hulston), pp. 109–113. Balkema.

Maurice P. A. and Namjesnik-Dejanovic K. (1999) Aggregate structures of sorbed humic substances observed in aqueous solution. *Environ. Sci. Technol.* **33,** 1538–1541.

McCarthy J. F., Williams T. M., Liang L. Y., Jardine P. M., Jolley L. W., Taylor D. L., Palumbo A. V., and Cooper L. W. (1993) Mobility of natural organic-matter in a sandy aquifer. *Environ. Sci. Technol.* **27,** 667–676.

McKnight D. M., Bencala K. E., Zellweger G. W., Aiken G. R., Feder G. L., and Thorn K. A. (1992) Sorption of dissolved organic carbon by hydrous aluminum and iron oxides occurring at the confluence of

Deer Creek with the Snake River, Summit County, Colorado. *Environ. Sci. Technol.* **26,** 1388–1396.

Meier M., Namjesnik-Dejanovic K., Maurice P. A., Chin Y.-P., and Aiken G. R. (1999) Fractionation of aquatic natural organic matter upon sorption to goethite and kaolinite. *Chem. Geol.* **157,** 275–284.

Murphy E. M., Zachara J. M., Smith S. C., and Phillips J. L. (1992) The sorption of humics to mineral surfaces and their role in contaminant binding. *Sci. Total Environ.* **117/118,** 413–424.

Murphy E. M., Zachara J. M., and Smith S. C. (1990) Influence of mineral-bound humic substances on the sorption of hydrophobic organic compounds. *Environ. Sci. Technol.* **24,** 1507–1516.

Namjesnik-Dejanovic K. and Maurice P. A. (in press) In-solution imaging of NOM single molecules and aggregates adsorbed to clay mineral surfaces. *Geochim. Cosmochim. Acta*.

Namjesnik-Dejanovic K., Maurice P. A., Aiken G. R., Cabaniss S., Chin Y.-P., and Pullin M. J. (2000) Adsorption and fractionation of a muck fulvic acid on kaolinite and goethite at pH 3.7, 6, and 8. *Soil Sci.* **165,** 545–559.

Ochs M., Cosovic B., and Stumm W. (1994) Coordinative and hydrophobic interactions of humic substances with hydrophilic Al_2O_3 and hydrophobic mercury surfaces. *Geochim. Cosmochim. Acta* **58,** 639–650.

Parfitt R. L., Fraser A. R., and Farmer V. C. (1977) Adsorption on hydrous oxides. III. Fulvic acid and humic acid on goethite, gibbsite and imogolite. *J. Soil Sci.* **28,** 289–296.

Schwertmann U. and Cornell R. M. (1991) *Iron Oxides in the Laboratory: Preparation and Characterization*. VCH.

Sposito G. (1984) *The Surface Chemistry of Soils*. Oxford University Press.

Steelink C. (1985) Implications of elemental characteristics of humic substances. In *Humic Substances in Soil, Sediment, and Water: Geochemistry, Isolation, and Characterization* (eds. G. R. Aiken, D. M. McKnight, R. L. Wershaw, and P. MacCarthy), Chapt. 18, pp. 457–476.

Stevenson F. J. (1994) *Humus Chemistry—Genesis, Composition, Reactions*. 2nd Ed. Wiley Interscience.

Stumm W. (1992) *Chemistry of the Solid-Water Interface*. Wiley.

Tipping E. (1981) The adsorption of aquatic humic substances by iron oxides. *Geochim. Cosmochim. Acta* **45,** 191–199.

Tipping E. and Cooke D. (1982) The effects of adsorbed humic substances on the surface charge of goethite (α-FeOOH) in freshwaters. *Geochim. Cosmochim. Acta* **46,** 75–80.

Tomaic J. and Zutic V. (1988) Humic material polydispersity in adsorption at hydrous alumina/seawater interface. *J. Colloid Interface Sci.* **26,** 482–492.

Traina S. J., Novak J., and Smeck N. E. (1990) An ultraviolet absorbance method of estimating the percent aromatic carbon content of humic acids. *J. Environ. Quality* **19,** 151–153.

Vermeer A. W. P. and Koopal L. K. (1998) Adsorption of humic acids to mineral particles. 2. Polydispersity effects with polyelectrolyte adsorption. *Langmuir* **14,** 4210–4216.

Vermeer A. W. P., van Riemsdijk W. H., and Koopal L. K. (1998) Adsorption of humic acids to mineral particles. 1. Specific and electrostatic interactions. *Langmuir* **14,** 2810–2819.

Wang L., Chin Y.-P., and Traina S. J. (1997) Adsorption of (poly)maleic acid and aquatic fulvic acid by goethite. *Geochim. Cosmochim. Acta* **61,** 5313–5324.

Yau W. W., Kirkland J. J., and Bly D. D. (1979) *Modern Size Exclusion Chromatography*. Wiley.

Zhou Q., Cabaniss S. E., and Maurice P. A. (2000) Considerations in the use of high-pressure size exclusion chromatography (HPSEC) for determining molecular weights of aquatic humic substances. *Water Research* **34,** 3505–3514.